The effects of diffusion depth and heat-affected zone in NE-GMAW process on SUH 310S steel using an Image processing method

H. Tagimalek *[1], M. Azargoman [2], M. R. Maraki [3], M. Mahmoodi [4]

[1,2,4] Faculty of Mechanical Engineering, Semnan University, Semnan, Iran
[3] Department of Materials and Metallurgy Engineering, Birjand University of Technology, Birjand, Iran

Abstract

In this research, the effect of diffusion depth and Heat-Affected Zone (HAZ) in Nanoparticles-Electrode Gas Metal Arc Welding (NE-GMAW) process with carbon dioxide protection on Heat Resistance Steel (SUH 310S) were investigated using the Image Processing (IP) and simulation software. Welding speed (S), Wire feed rate (F) and Voltage (V) as effective parameters were considered for experimental tests. The Design of Experiment (DoE) was using the Taguchi method with L11 array without experiment replication. According to the Scanning Electron Microscope (SEM) images of the experiments, changes in three effective parameters were obtained. The voltage and wire feed rate had the most significant impact on increasing HAZ zone and ultimately the diffusion depth due to the increase of heat generated and the creation of a more comprehensive Weld Pool (WP). The experiments with 11-samples were used to find the diffusion depth and surface zone of the HAZ region by NI vision IP software. The effect of parameters in image processing and simulation software in results showed validation for evaluating changes in HAZ zone.

Keywords: Gas metal arc welding, Heat resistance steel, Heat-affected zone, Diffusion depth, Image processing.

1. Introduction

Heat resistance steel is one of the most widely used metal materials in various industries such as petroleum and petrochemical, land transportation and chemical industries [1]. In heat resistance steels, when the chromium content increases, properties such as toughness and weldability decrease, and the strength increases [2]. For this purpose, extensive research has been carried out by welding researchers to investigate the solidification of weld metal, microstructure and heat-affected zone of phase transforms and welding discontinuities [3]. The Gas Metal Arc Welding (GMAW) process, due to its high permeability, the ability to connect sections of various thicknesses and with high machining capability, is now used widely in the pipeline, pipeline manufacturing, and automotive industries [4]. Nowadays GMAW is one of the low cost and high performance joining methods widely used in industry [5]. The schematic of the NE-GMAW process was shown in Fig 1. In this welding process, thermal plasma was produced between the electrode and the workpiece. NE-GMAW process has high-quality compared to the GMAW welding method due to its proper flow of fluid in the welding pool. The primary function of the protective gas in this process

**Corresponding author*
Email:h_tagimalek@semnan.ac.ir
Address: Faculty of Mechanical Engineering, Semnan University, Semnan, Iran
1. PhD Student
2.PhD Student
3. Lecturer
4. Assistant Professor

was to protect the melted metal in the pool from atmospheric nitrogen and oxygen present in form of the welding pool [6]. Besides protective gas enables the task of creating a uniform and stable arc of high-quality metal transfer and increases productivity [7]. The GMAW process, wire feed rate (F), welding speed (S), and voltage (V) were significant factors affecting surface quality, diffusion depth, and weld joining. The mechanical properties of the weld were highly dependent on the geometry so that the geometry of the weld was directly related to the quality and stability of the weld created in the structures. One of the requirements to obtain an acceptable weld geometry was that there should be a weld between the base metal and the electrode because the base metal has to be melted sufficiently to form the grain to the desired depth. For this reason, diffusion depth was one of the most important parameters in welding. Also, the GMAW process must be controlled by maintaining proportionality between width and height of the weld geometry to reach the proper depth of diameter of consumed electrode and created arc [8].

Wang et al. [9] studied the microstructure formation and precipitation in laser welding of micro-alloyed C-Mn steel. The results showed that the heat-affected zone consisted of both ferrite and martensite/austenite island, found in both of fine-grained heat-affected zone and the mix-grained heat-affected zone. Ramazani et al. [10] studied the impact of GMAW welding parameters on the diffusion depth of two-phase steels. In addition to investigating other diffusion depth capabilities, they studied the influence of diffusion depth on the mechanical properties of the weld. In the heat-affected zone, the microstructure varied from bainite to coarse-grained ferrite and tempered martensite. Kaiyuan et al. [11] in a study investigated the effect of single and binary pulses on the structure and mechanical properties of welding joints during GMAW with high-power binary wires. Experimental results showed that through single-wire two-pulse GMAW, stable welding could be obtained. Also, high-quality welding geometry was obtained with partial spraying, without porosity or bulge. In a study, Yan et al. [12] investigated the influence parameters at diffusion depth that had a direct relevance with quality and strength of the weld. In addition to controlling the parameters affecting on diffusion depth of significance between the grain shapes, they also studied the information obtained from welding region using an image processing system. Finally, by measuring the melt volume, specific parameters were obtained to enhance diffusion depth. They proposed a welding voltage measurement method to improve and ensure diffusion conditions at the beginning of the welding. Accordingly, the two-second arc was given to the workpiece to simulate welding. The maximum voltage changes in the current were determined to describe the diffusion of the weld. The results indicated that the wire feed rate had little effect on the diffusion state. The workpiece had two states at welding time, the first includes welding pool growth and the second part shows stable welding with stability in the parameters. The final result showed that by controlling the turning point and comparing it with the obtained data, the diffusion depth could be mastered. Zhu et al. [13] studied the behavior of molten pools and their effect on welding defects in the narrow gap by the GMAW method in Al 5083 using a three-dimensional simulation. Three different weld geometry levels have been obtained that do not have the same flow patterns due to thermal differences and other forces. The results show that the upward fluid flow causes non-fusion defect at the edges of the welding geometry and the downward fluid flow constitutes porosity. In a study, Marcan et al. [14] investigated welding of two different metals of aluminum alloys with the GMAW method. During the investigation, tensile and hardness tests were carried out, which resulted in an increase in tensile strength up to 90% and an increase in amount of corrosion at the welded zone. Huang et al. [15] investigated the metallurgical and mechanical properties of magnesium-aluminum alloy welded by GMAW with different plate thicknesses. They considered that the thickness of plates is a useful parameter. They obtained results that showed the higher plate thickness due to higher surface heat and more hydrogen uptake of porosity. Also, the high thickness increases grain-size and decreases resistance. The GMAW is a multi-energy process involving various physical and chemical phenomena, such as physical plasma, heat flow, and metal transfer fluidity [16]. The function of GMAW is to create an arc between the electrode that continuously feeds and creates a weld pool. This range is protected by an external (neutral or active) gas. The heat is generated by the arc melts the base metal surface and electrode tip after that it's formed during the mixing of the electrode and the base metal [17].

In this research, wire feed rate, welding speed, and voltage were considered as effective input parameters of process. The amount of parameter changed with Nano-silica in diffusion depth and the HAZ zone according to research requirements. In the present study, after empirical tests, Simulation, NE-GMAW sample using SEM microscopy and Image processing (IP) method studied.

2. Materials and Methods

The purpose of this research was using image processing and numerical computation method to investigate the influence of effective parameters on microstructure of the heat-affected zone in neutral gas welding and evaluation of this zone. For this purpose, as shown in Fig. 2, NE-GMAW process devices Including the Carry MIG 501 wire feed system and FP4M machine.

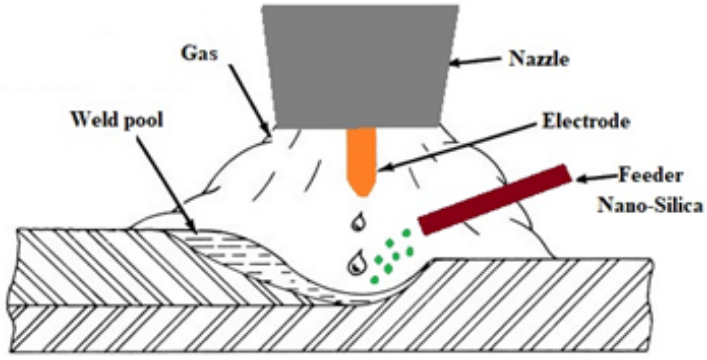

Fig. 1. Schematic of the Nanoparticles - Electrode Gas Metal Arc Welding (NE-GMAW).

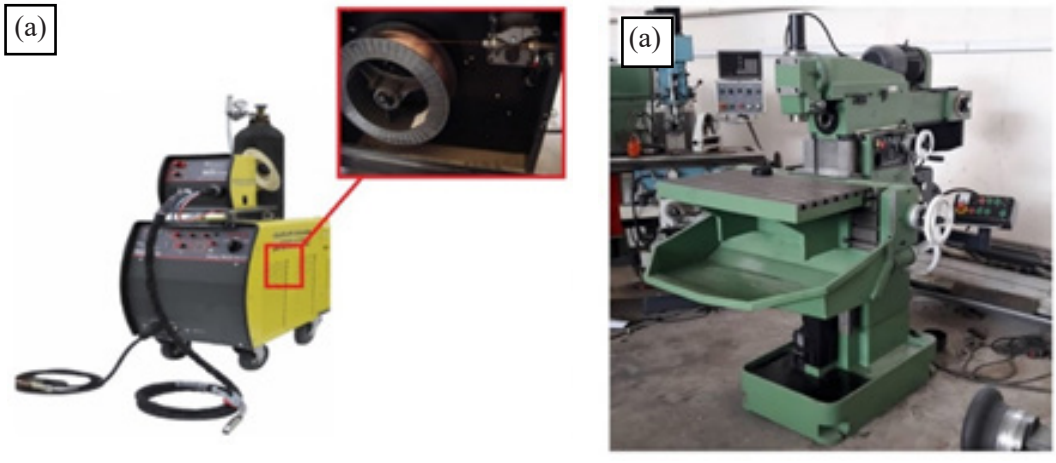

Fig. 2. GMAW devices; a) Carry MIG 501, b) FP4M machine.

Referring to the above, in the present study, 11 experiments were carried out on heat resistance steel (SUH 310S) with the presence of Nano-silica on dimensions of 10×30×50 mm^3, as a base metal in NE-GMAW welding. Structure of the SUH 310S chemical and mechanical is given in Tables 1 and 2. Table 3 shows the input parameters in the NE-GMAW process.

Table 1. Chemical composition of SUH 310S steel.

Metal	Fe	C	Mn	P	Si	Cr	Ni
Weight (%)	Bal	0.10	2.00	0.05	2.50	25.00	21.00

Table 2. Mechanical properties of SUH 310S steel.

Mechanical properties	TS (MPa)	YS(MPa)	Elongation (%)	Hardness (HB)
Value	524	217	40	225

In this experiment, a feeding wire electrode AWS/ ASME ER 309, with a diameter of 1 mm was used. The chemical composition of the consumable electrode AWS/ASME ER 309 is shown in Table 4. Carbon dioxide gas was used as a protective gas. Changes in the parameters of voltage, welding speed, and wire feed rate on microstructure of diffusion depth and heat-affected zone are investigated. Fig. 3 showed the NE-GMAW experimental samples.

After the empirical test, workpieces were cut and prepared for etching (visualization of the heat-affected zone). Workpieces was imaged by using the SEM microscope at Razi Metallurgical Research Center in the Islamic Republic of Iran.

3. Simulation

Weld simulation was carried out in Abaqus software by applying mesh modification around the weld pool in Abaqus software. Master model design was implemented in Solid work software. Welding simulation process with the electrode was continuous and according to the standard. The FE model consists of thermal and mechanical properties of base metal and the weld electrode as a function of temperature. Modeling such as mesh adaptation during the process and mesh of welding and thermal source movement was used. Finally, weld geometry and area of the heat-affected zone were investigated by this software. Prediction of weld geometry shows that the numerical results and experimental measurements have good agreement with each other and existing model. Fig. 4 shows the simulation results of NE-GMAW process on SUH 310S for to validation of weld geometry with Abaqus software. The results show a high percentage of compatibility between empirical test and simulation.

Table 3. Input parameters of NE-GMAW process.

Parameter NE-GMAW	Voltage (V)	Wire Feed Rate (cm/min)	Welding Speed (mm/min)
Range	17 ~ 32	210 ~ 253	200 ~ 400

Table 4. Chemical composition of AWS/ASME ER 309 electrode.

Metal	Fe	C	Mn	P	Si	Cr	Ni	Cu
Weight(%)	Bal	0.03	1.50	0.01	0.65	21.00	12.00	0.70

Fig. 3. NE-GMAWed Experimental samples.

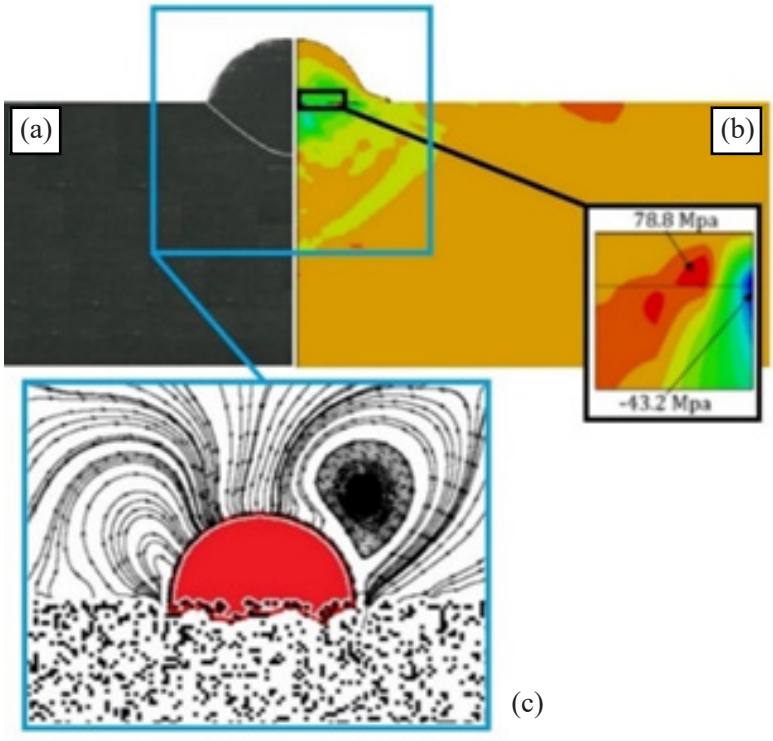

Fig. 4. An image of the cut section welding geometry after the NE-GMAW process; a) Experimental, b) Simulation and c) Flow carbon dioxide gas the Weld zone.

4. Microstructural

Fig 5, shows the SUH 310S microstructure. The existing lines show the complete separation of grain boundaries and also offer two ferrite and martensite phases. Therefore, an optimal combination of strength and ductility can be achieved a uniform distribution of martensite islands in the field of fine-grained ferrite. Thus, the conversion of austenite to martensite in test of steel happened gradually. Fig 6, shows the SEM microstructure Nanoparticles silica.

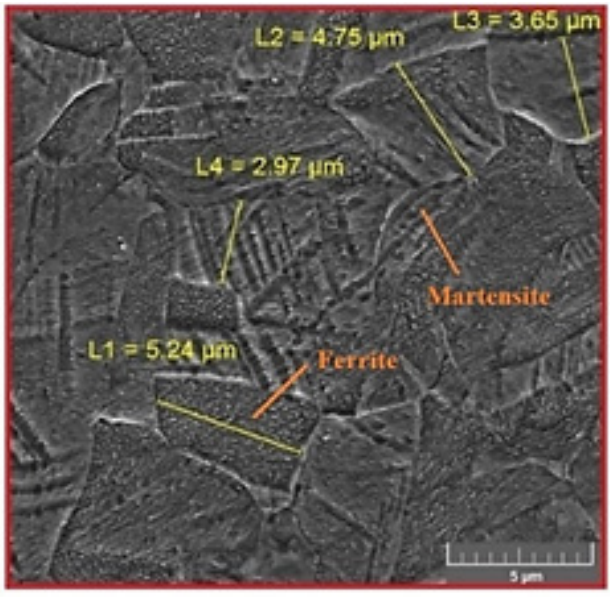

Fig. 5. Base metal (SUH 310S) microstructure.

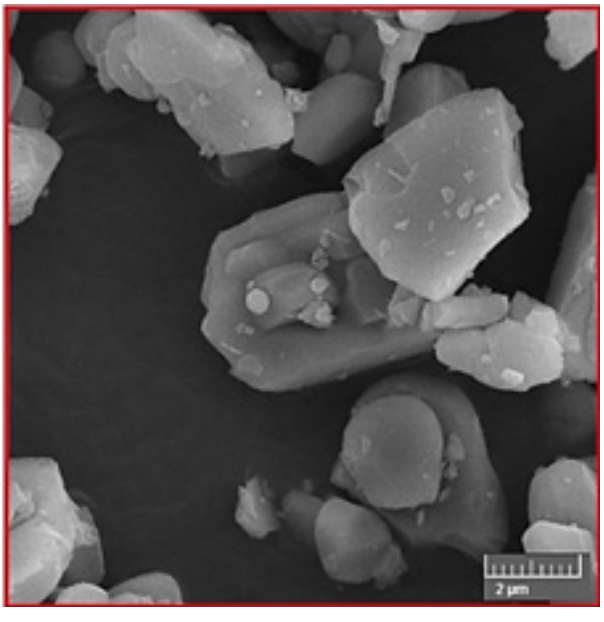

Fig. 6. SEM microstructure of Silica Nanoparticles.

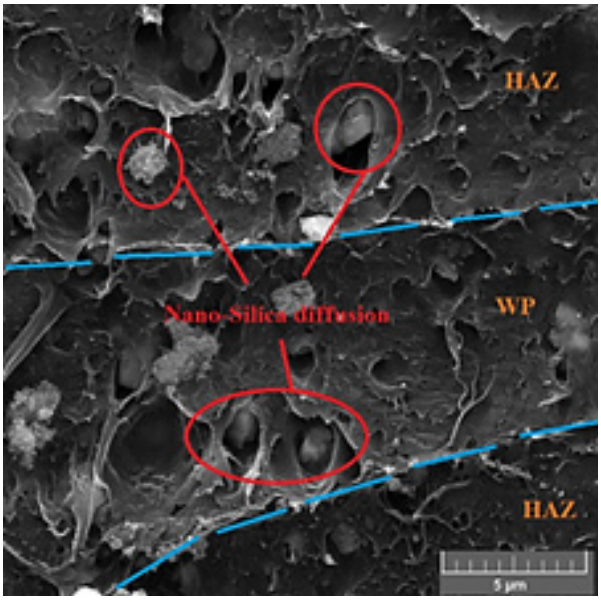

Fig. 7. The microstructure of nano-silica diffusion, heat-affected zone and weld pool.

The microstructural changes of weld pool and the heat-affected zone were investigated by varying the wire feed rate, welding speed, and voltage. The main task of protective gas was to protect the weld pool from nitrogen, oxygen in atmosphere and avoid porosity. Carbon dioxide gas in this method was decomposed into oxygen and carbon monoxide at the arc site. These gases were converted to carbon dioxide after cooling and were excreted before the boiling solid. For this reason, the porosity in the workpiece was reduced. And the use of carbon dioxide increases the volume fraction and weld pool (WP) diffusion depth. The welding pool has the highest temperature. In partially melted zone near the weld pool, ferrite is formed.

The welding nozzle of weld pool is transformed from austenite to ferrite + martensite. This is due to the cooling of carbon dioxide gas and the presence of silica nanoparticles in molten pool to accelerate the transformation of ferrite. Weld metal separation line was partially melted and the heat-affected zone was quite clear. According to Figs 8a and 8b obtained from the welded zones in the experiment, wire feed rate unlike parameters had little effect on microstructure of the base metal but had the most significant impact on changing

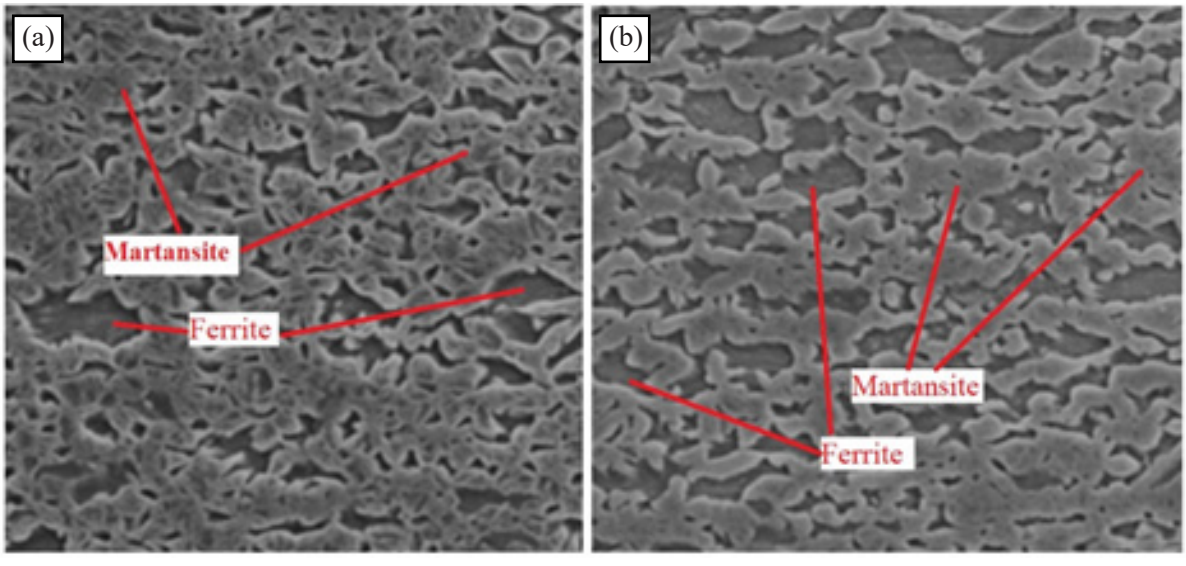

Fig. 8. SEM images; a) heat-affected zone and b) weld pool.

dimensions and size of weld geometry. The heat is produced directly related to current, voltage and also was inversely related to the welding speed. As the welding voltage increases, arc length and diffusion rate increase and the stability of arc fluctuates as the temperature increases. Due to those above, the rate of welding spray and porosity increase in the welding pool. It should be noted that in this study, the discharge of gas depends on the voltage range determined for all welded samples.

5. Cross-sectional zone imaging

Machine vision and image processing were used to measure output parameters. DFK-23gm021 camera with 60 fps data rate, 1280×960 resolution with CCD sensor, m1614-mp2 lens system and 30 mm diameter and 12 mm focal length was used to imaging. For beginning calibration must be performed to resolve errors in visualization system. Error factors such as position vector and camera rotation matrix were compared with general coordinates. Since the camera is fixed, only one calibration was performed. In this study, camera was imaged in different directions to calibrate all conditions (Fig. 9). A 10 mm gauge with an accuracy of 0.001 mm was used to verify machine vision performance and system calibration. The results of this validation are presented in Table 5. After machine vision, images were analyzed using MATLAB software.

Experiments, imaging, and image processing on the sample and obtaining desired outputs such as heat-affected zone (A), diffusion depth (H), along with the Taguchi design experiments [18] are reported in Table 6. Results show that heat produced during and after the process is higher in inner radius than in outer radius. This temperature difference causes the temperature gradient along radius to be significantly influenced by heat-affected zone. To find the HAZ region, a welded sample was used to numerically solve the geometry. The results are presented in Table 6 along with the image processing results.

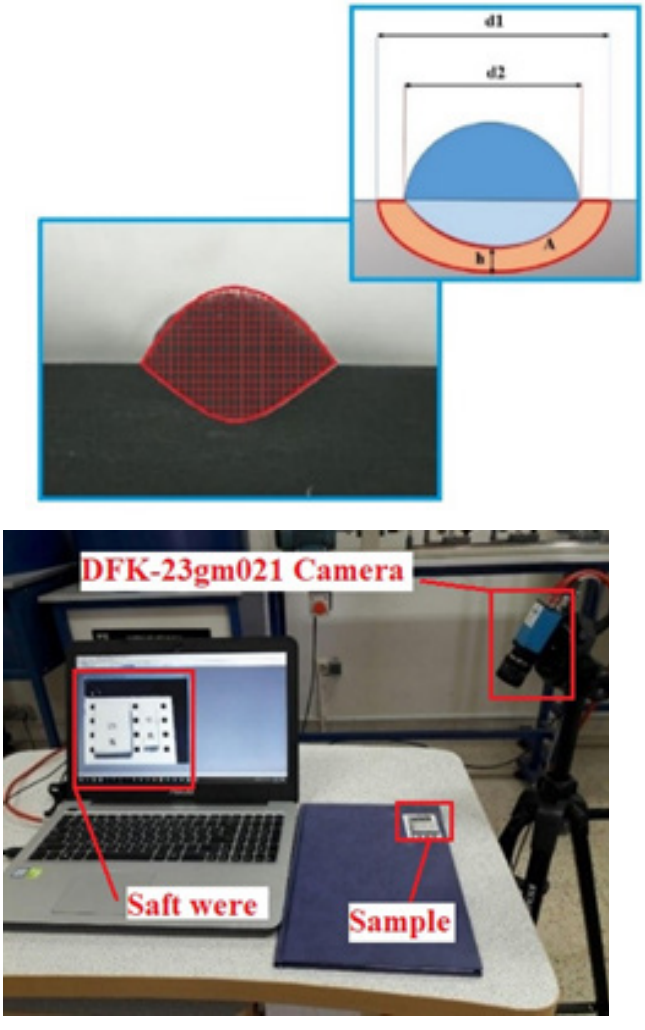

Fig. 9. Image processing method of the cut section; a) classification of the weld geometry by NI vision software and b) block gauges for verification and modeling.

Table. 5. Gauge Block Validation Results.

	Accuracy (mm)	Nominal size (mm)	measurement value	Error rate
Gage bloc	0.001	10	9.93	0.07

Table. 6. Results design of experiments of numerical calculations (NC) and image processing (IP).

Numerical computing outputs		Image processing software outputs		effective parameters			Ex
diffusion depth (mm)	heat-affected zone (mm)	diffusion depth (mm)	heat-affected zone (mm)	Welding speed (mm/min)	Voltage (V)	Wire feed rate (Cm/min)	
1.98	5.67	1.28887	5.51569	Fix	Fix	210	1
1.54	16.26	1.60742	15.16703	Fix	Fix	231	2
1.99	26.05	2.09489	23.39566	Fix	Fix	252	3
1.78	5.01	1.12396	4.96536	Fix	17	Fix	4
1.45	9.05	1.33118	8.95209	Fix	22	Fix	5
1.98	9.53	1.38901	9.33676	Fix	27	Fix	6
1.51	14.55	1.48332	13.82142	Fix	32	Fix	7
2.25	11.39	2.19025	11.34478	200	Fix	Fix	8
1.78	10.63	1.77001	10.63893	250	Fix	Fix	9
1.89	8.80	1.71823	8.63060	315	Fix	Fix	10
2.30	11.36	2.29918	11.30916	400	Fix	Fix	11

6. Heat-affected zone and diffusion depth

HAZ and diffusion depth have the most influence on residual stresses in welding sample. The gap between electrode and sample can reduce the HAZ and diffusion depth. For this purpose, there is an optimal limit for a gap, heat-affected zone, and diffusion depth. In this study, in addition to investigating the effect parameters on heat-affected zone, image processing on increasing or decreasing the heat-affected zone was also investigated.

Figs 10 shows that increasing parameters of voltage and wire feed rate cause an increase in the heat-affected zone. Conversely, as the welding speed increases, heat-affected zone decreases significantly.

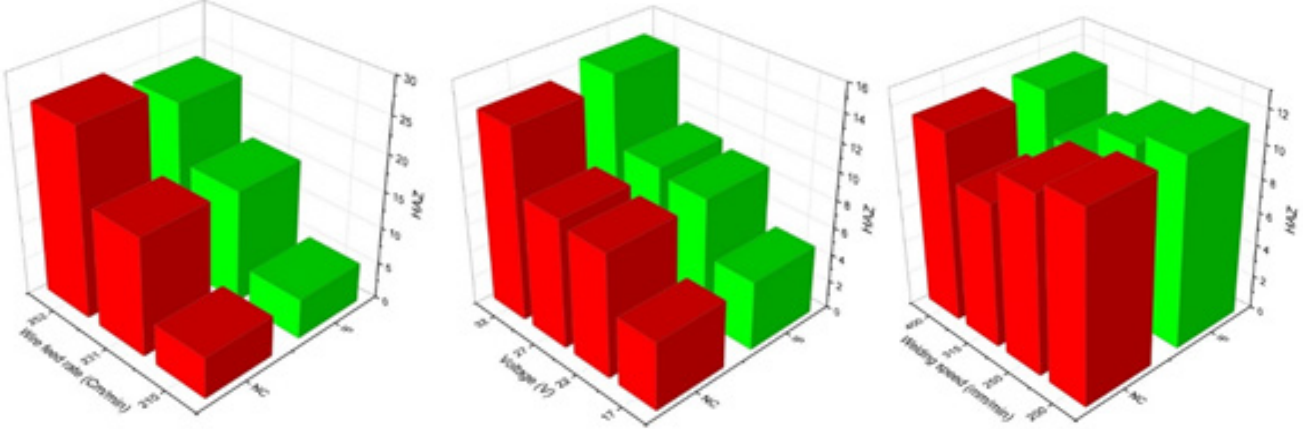

Fig. 10. Effect of effective parameters on the heat-affected zone of numerical calculations and image processing

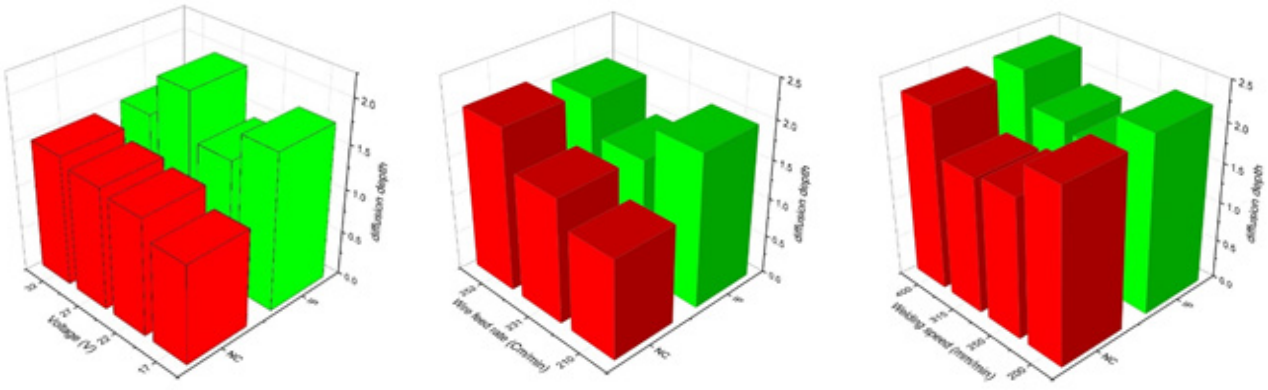

Fig. 11. Effect of effective parameters on the diffusion depth of numerical calculations and image processing.

Figs 11 shows that the diffusion depth increases by improving two parameters of voltage and wire feed rate, which are the main factors in increasing the temperature in welding pool. Conversely, in these two parameters, the diffusion depth with a gentle slope decreases by increasing welding speed. It is important to note that high voltages are directly related to the weld spraying phenomenon. At high voltages, protective gas discharge should be increased to avoid splashing in welding zone.

7. Conclusion

In this study, diffusion depth and heat-affected zone in Nanoparticles - Electrode Gas Metal Arc Welding (NE-GMAW) were investigated to change weld geometry and thermal effects using image processing and simulation. Input parameters including welding speed, wire feed rate, and voltage were verified using experimental tests that was performed and results showed high accuracy of the tests.

- According to microstructural images, if the Co_2 gas is used in the NE-GMAW process, volume fraction and diffusion depth increase.
- Increasing the wire feed rate increases the amount of melt in pool and the heat transfer in weld zone which resulting in coarser grains and in mixing Nano-silica in welding zone and inclusion zone.
- At most experiments, a slight deviation of the arc is observed, which is considered a negative parameter.
- Increasing the voltage and wire feeding rate parameters increases heat-affected zone and vice versa as the welding speed increases in heat-affected zone, decreases significantly.
- Two parameters of voltage and wire feed rate, which are main factors in increasing the temperature in welding pool zone, increase the diffusion depth.
- An increased in voltages leading to welding melt spraying, a high discharge of protective gas should be used to avoid porosity of the weld zone.
- Depending on images and diagrams generated by image processing, as the welding speed increases, the diffusion depth decreases with a gentle slope.

8. Author Contributions

Tagimalek (40%) and Azargoman (25%) planned the scheme, initiated the project, and suggested the experiments; Tagimalek and Maraki (15%) conducted the experiments and analyzed the empirical and simulation results; Tagimalek and Mahmoodi (20%) developed the mathematical modeling and examined the theory validation. The manuscript was written through the contribution of all authors. All authors discussed the results, reviewed and approved the final version of the manuscript.

9. Acknowledgments

The authors are very much thankful to the unknown reviewers for their valuable and constructive suggestions which improved the readability of the paper.

10. Conflict of Interest

The authors declared no potential conflicts of interest for the research, authorship, and publication of this article.

11. Funding

The authors received no financial support for the research, authorship, and publication of this article.

Reference

[1] G. Li, B. Jiang, H. Liu, L. Ning, D. Yi, X. Wang, Z. Liu: Pro. Org. Coat., 137(2019),105315.
[2] Y. Peng, L. Yu, Y. Liu, Z. Ma, H. Li, C. Liu, J. Wu: Mater. Sci. Eng. A., 767(2019),138419.
[3] R. Zong, J. Chen, C. Wu: Jour. Mater. Pro. Tech.,

285(2020),116781.
[4] Y. Han, J. Tong, H. Hong, Z. Sun: The. Inter. Jour. Ad. Manu. Tech., 101(2019), 993
[5] B. Wu, Z. Qiu, Z. Pan, K. Carpenter, T. Wang, D. Ding, S.V. Duin, H. Li: Jour. Mater. Sci. Tech., 52(2020), 231.
[6] C. Chen, S. Lin, C. Fan, C. Yang, L. Zhou: The. Inter. Jour. Ad. Manu. Tech., 97(2018), 3621.
[7] T. Xiang, H. Li, Y. Geo, S.Y. Zhao, L.Y. Lou, H. Wang: The. Inter. Jour. Ad. Manu. Tech., 102(2019), 862.
[8] K. Wu, P. Xie, Z. Liu, M. Zeng, Z. Liang: Jour. Manu. Pro., 49(2020), 434.
[9] X.N. Wang, C.J. Chen, H.S. Wang, S.H. Zhang, M. Zhang, X. Luo: Jour. Mater. Pro. Tech., 226(2015), 110.
[10] A. Ramazani, K. Mukherjee, A. Abdurakhmanov, U. Prahl, M. Schleser, U. Reisgen, W. Bleck: Mater. Sci. Eng. A., 589(2014), 12.
[11] K. Wu, N. Ding, T. Yin, M. Zeng, Z. Liang: Jour. Manu. Pro., 35(2018), 732.
[12] Z.H. Yan, G.J. Zhang, H.M. Gao, L. Wu: Sci. Tech. Weld. Join., 10(2013), 747.
[13] C. Zhu, J. Cheon, X. Tang, S.J. Na, H. Cui: Inter. Jour. Heat. Mass. Tran., 126(2018), 1218.
[14] E. Mercan, Y. Ayan, N. Kahraman: Eng. Sci. Tech. An. Inter. Jour., 23(2020), 730.
[15] L. Huang, X. Hua, D. Wu, Z. Jiang, Y. Ye., Jour. Manu. Pro., 37(2019), 443.
[16] T. Kannan, J. Yoganandh: The. Inter. Jour. Adv. Manu. Tech., 47(2010), 1093.
[17] D. Yang, G. Wang, G. Zhang: The. Inter. Jour. Adv. Manu. Tech., 19(2017), 2081.
[18] M.R. Maraki, H. Tagimalek, M. Azargoman, H. Khatami, M. Mahmoodi: Inter. Jour. Engin., 33(2020), 2524.